J. Membrane Biol. 50, 43–63 (1979)

Complex Admittance of Na^+ Conduction in Squid Axon

H.M. Fishman*, D. Poussart**, and L.E. Moore*

Marine Biological Laboratory, Woods Hole, Massachusetts 02543

Received 16 February 1979; revised 29 May 1979

Summary. The complex admittance, $Y(p)$, of squid axon was measured (4–1000 Hz) during step voltage clamp to obtain linear data on Na^+ conduction. $Y(p)$ is used as a spectroscopic tool to identify Na^+ and K^+ conduction, which dominate $Y(p)$ at low frequencies and can be separated from each other and from the static capacitance. Na^+ conduction is readily distinguishable from K^+ conduction in that it produces a steady-state negative conductance. The admittance of the Na^+ system can show an anomalous resonance or an antiresonance depending on whether the net shunt conductance is negative or positive. Use of the Na^+ negative conductance to neutralize leakage yields a measurement of dielectric capacitance at low frequency. A 90° phase angle suggests that the capacitance is ideal.

In previous publications (Fishman, 1975; Fishman, Moore & Poussart, 1977*b*; Fishman *et al.*, 1977*c*; Poussart, Moore & Fishman, 1977) the utility and importance of rapid, low-frequency measurements of the complex impedance/admittance of the squid axon was demonstrated. At low frequencies (< 1000 Hz), the ion conduction processes dominate the admittance and the effect of membrane capacitance is minimal (Cole, 1972; Fishman *et al.*, 1977*c*; Poussart *et al.*, 1977). Consequently the low frequency admittance contains information about the linear properties of ion conduction which can be compared directly with any linear model. Furthermore, the use of present day techniques of digital signal processing together with internal electrodes results in effective use of experimental time. Consequently, detailed measurements of the complex admittance during step voltage clamps are possible. Since a four-electrode measurement (two for voltage and two for current) (Cole, 1977) is compatible with these methods, the admittance can, in principle, be determined accurately at low frequencies without corrections for electrode characteristics.

* *Permanent address and for reprint requests:* Department of Physiology and Biophysics, University of Texas Medical Branch, Galveston, Texas 77550.

** *Permanent address:* Department de Genie Electrique, Universite Laval, Quebec, Canada.

0022-2631/79/0050-0043 $04.20

The objective in the present experiments is to study the squid axon admittance under conditions in which the Na^+ conduction system is operative and the K^+ conduction system is suppressed. We have reported preliminary admittance measurements on the Na^+ system (Fishman *et al.*, 1977*c*; Poussart *et al.*, 1977; Fishman, Poussart & Moore, 1978). These data are important for comparison with linear kinetic models such as the linearized Hodgkin-Huxley (ℓHH) equations (1952) and are useful for comparison with the description of kinetics obtained from analysis of spontaneous conductance fluctuations. In addition, the Na^+ system produces a steady-state negative conductance, and the complications arising from such an element need to be described.

Materials and Methods

Most of the experimental details were described previously (Fishman *et al.*, 1977*c*; Poussart *et al.*, 1977). That is, the preparation, chamber, regulation of solution flows, internal axial electrodes, voltage clamp system, and technique for internal perfusion were the same. In addition, external solutions were cooled by means of an ice bath to assure noise-free operation. Also, the chamber, solutions, and sensitive circuits were all contained in an aluminium cage to minimize electrostatic effects.

The external current electrodes consisted of platinum-black platinum sheets (4×4 mm); a pair for guards on both sides of a central sheet. A transresistance operational amplifier was used to convert the central current to a proportional output voltage. Because of a more favorable signal-noise condition (Fishman *et al.*, 1977*c*), unguarded current measurements were also made with just the central sheet in a partitioned chamber. The central region contained the flowing seawater (SW) and the adjacent partitioned regions served as air gaps (5 mm in length). The axon in the air gaps was "deactivated" by approaching the axon with a heated nichrome wire until "notches" in the clamp currents were imperceptible to the eye. The dead ends constituted a shunt on the central region, but the apparent leakage increase never exceeded twice the original leakage and was a good comprise in that it eliminated obvious instabilities in the ends which were observed as current injected into the central region. All of the results presented have been corroborated by both methods of current measurement. Two criteria have been established for assuring that the measured current is essentially that from the region of axon under uniform potential control. (i) The admittance measured under voltage clamp must be the reciprocal of the impedance measured under current clamp conditions. (ii) The spectrum of the current response under voltage clamp must be "white" when the recorded voltage response to a "white" noise current clamp is applied as a command to the voltage-clamp system. The latter criterion is a very stringent requirement. It tests the assumption that the measured transfer function is invariant with respect to either controlled variable since any instabilities or aberrations occurring during the control of the current are unlikely to be exactly the same during the control of voltage, if the measured response depends upon a third variable as well (e.g., some spatial variable).

All of the admittance measurements were done during voltage-clamp conditions using a broadband signal (pseudorandom noise) source and discrete Fourier transform techniques (Poussart *et al.*, 1977). The perturbation signal was generated from a read-only memory

in which the digital values of a low-pass filtered, synchronized binary sequence had been stored. The measurement band was usually 4–1000 Hz, and a sample record consisted of 1024 digitized points, acquired in a 250 msec interval, 250–500 msec after the onset of a step change in potential. Thus "steady-state" in this paper is defined as this measurement time "window". The admittance, free of aliasing, was plotted as 256 frequency points with smoothing to obtain magnitude, $|Y|$, and phase, ϕ, functions simultaneously on two XY recorders. A complex admittance plot may be useful but has not been implemented. The reference measurements of $|Y|$ and ϕ were derived from a pure resistor which was substituted for the preparation, a procedure that effectively compensated for the residual frequency dependence of the clamping system. The emphasis was on low frequency behavior. These was no compensation for series resistance (about $7\Omega \cdot cm^2$) since the membrane impedance exceeded the series resistance by more than an order of magnitude at all frequencies and under all conditions of measurement (*see* $|Y|$ in Fig. 1) in these experiments.

The calculations of the complex admittance from the *l*HH model was done on a Digital Equipment Corporation PDP-11/70 computer. The program implemented Eqs. (1), (1*a*), (1*b*), and (1*c*) and parameters given in Fishman *et al.* (1977*c*)[1]. The complex admittance is available as $|Y|$ and ϕ at 300 frequency points in any specified frequency range. Both functions can be plotted on the CRT of a terminal with either automatic or forced scaling. Alternatively, the plots are available on a Versatec printer/plotter or in tabular form. A listing of the program is available (HMF).

Results

1. Identification of K^+ and Na^+ Conduction in the Admittance

In previous experiments (Fishman *et al.*, 1977*c*; Poussart *et al.*, 1977) it was possible to distinguish between K^+ conduction and Na^+ conduction in the admittance by suppressing one or the other of these systems. Figure 1 illustrates this point with data from an experiment on a single axon in which the various ion conduction processes are systematically suppressed through a sequence of changes of the inside and outside solutions. The curves in $|Y|$ and ϕ, labeled *1*, were obtained at rest potential (−58 mV) for an axon internally perfused with a buffered solution of 500 mM KF plus 5 mM Tris HCl and with SW flowing externally. A characteristic antiresonance occurs at about 150 Hz. After changing the internal perfusate to a buffered (pH = 7.5, 25 °C) solution of 50 mM KF plus 50 mM CsF (with sucrose to maintain a constant osmolarity), the curves labeled *2* were recorded at the new rest potential (−32 mV). Another antiresonance occurs that is distinguishable from curve *1* in that the antiresonant frequency shifted to 55 Hz; the antiresonance is much sharper; and the phase function shows an abrupt transition from

[1] The equation for temperature factor was incorrectly printed. It should be Q_{10} raised to the power $(T\text{–}6.3)/10$.

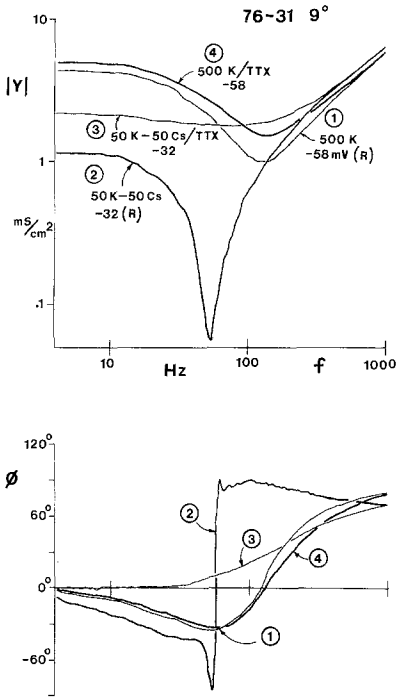

Fig. 1. Identification of K^+ and Na^+ conduction in the low frequency complex admittance of an internally perfused squid axon at rest potential (*R*). The complex admittance is plotted as magnitude and phase functions of frequency for a sequence of inside and outside solution changes that suppress one, the other, or both ion conduction processes. (*1*): Both K^+ and Na^+ are operative. (*2*): K^+ is suppressed; Na is operative. (*3*): Both K^+ and Na^+ are suppressed. (*4*): K^+ is operative; Na^+ is suppressed. Increase in $|Y|$ at low frequency (< 10 Hz) in going from curve *2* to *3* and curve *1* to *4* indicates a negative conductance has been removed from the measurement

$-90°$ to $+90°$. Several minutes after addition of TTX (1 μM) to the external SW with the same 50 K^+/50 Cs^+ perfusate, the antiresonance is almost completely abolished, producing the set of curves labeled *3*. Finally, the internal perfusate is switched back to 500 mM KF while maintaining TTX in the external SW. An antiresonance (*4*) similar to the initial one (*1*) reappears. From step voltage clamp data the conduction systems that are operative during the above sequence of internal and external solution changes are as follows: Curve *1*, both K^+ and Na^+; curve *2*, mainly Na^+ with suppressed K^+; curve *3*, both Na^+ and K^+ suppressed; and, curve *4*, mainly K^+ with suppressed Na^+. There were no significant changes in leakage during the solution changes. From the above it is apparent that (i) curve *4* reflects the interaction of the K^+ conduction system with membrane capacitance, (ii) curve *2* reflects

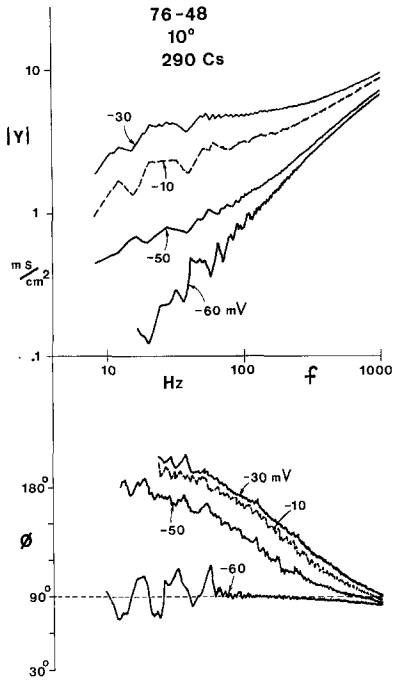

Fig. 2. The complex admittance of a squid axon internally perfused with a buffered solution of 290 mM CsF and at various absolute membrane potentials. Since K^+ conduction has been eliminated, the admittance is that of the Na^+ system, leakage and dielectric capacitance. At -10, 30 and 50 mV the $|Y|$ reflects a negative conductance since $\phi > 90°$. At -60 mV, Y resembles an ideal capacitance (lossless) with $\phi = 90°$ for $f < 250$ Hz

the interaction of the Na^+ conduction system with membrane capacitance, and (iii) curve 1 reflects the interaction of all ion conduction systems with membrane capacitance. Two additional points are of interest. The resting membrane admittance shown as curve 1 is mainly K^+ but does have a substantial contribution from the Na^+ system. Second, the suppression of the Na^+ conduction system results in an increased $|Y|$ (going from curve *2* to *3* or from curve *1* to *4*). The only way in which a block of a conductance can produce an increase in $|Y|$ is if that conductance is negative before the block.

2. A Negative Na^+ Conductance

From the data in Fig. 1, a negative Na^+ conductance is inferred from the behavior of Y before and after the block of $\bar{g}_{Na}$. From the phase function of curve *2* in Fig. 1, it is apparent that the phase does

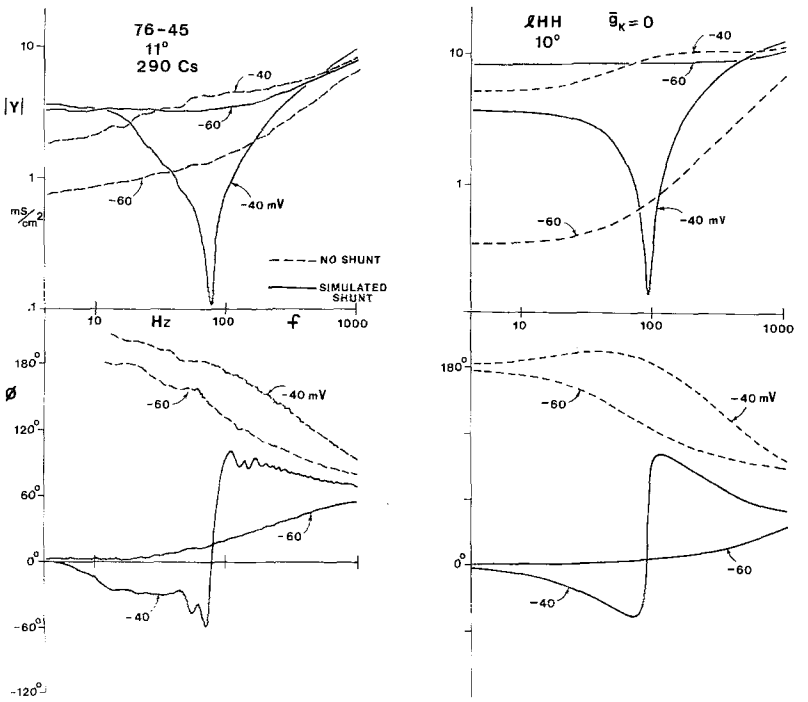

Fig. 3. Comparison of the complex admittance measured in a squid axon (left) with a calculation from the ℓHH model (right) with parameters that take into account the experimental conditions. No antiresonance occurs in Y at -60 or -40 mV (dashed curves); however, after simulation of a positive shunt conductance to make the net shunt conductance positive ($\phi \leqq \pm 90°$) experimentally (*see* text) and in the ℓHH model, antiresonance appears at -40 mV (solid curves). In the ℓHH calculations the h parameter has been restricted to take on values ≥ 0.1 (with potential) corresponding to partial removal of Na^+ inactivation during Cs^+ perfusion. A series resistance of $7\,\Omega \cdot cm^2$ was used in the calculations. All other parameters are standard HH. Potentials are absolute

not exceed $\pm 90°$, and consequently there is sufficient positive conductance (from residual K^+ conduction and leakage) under the conditions of measurement to obscure the negative conductance behavior. In order to obtain and observe a net shunt negative conductance, outward K^+ conduction was completely suppressed by perfusion with a buffered (pH = 7.5 @ 25 °C) solution of 290 mM CsF plus sucrose without any K^+. These data are shown in Fig. 2. The most obvious aspect of the admittance data in Fig. 2 in comparison to curve *2* in Fig. 1 is that an antiresonance does not occur. Nevertheless, the low frequency data for potentials -10, -30 and -50 mV clearly show phase $\geqq 180°$ which means that the $|Y|$ functions for these potentials reflect a net negative conductance, which was expected from the Na^+ data in Fig. 1. The apparent paradox of the antiresonance stems from the nature of a nega-

tive conductance element. The admittance function of a circuit with two or more different susceptive elements containing both positive and negative shunt conductance elements can produce an antiresonance or no antiresonance depending upon whether the net shunt conductance is either positive or negative. (*See Discussion* for further explanation). To illustrate this point the admittance was measured in an axon internally perfused with 290 mM Cs^+. As shown in Fig. 3, the dashed curves in the left-hand side of the figure reproduce the data in Fig. 2 at two different potentials (-40 and -60 mV). A pure positive conductance across the membrane was then simulated by injecting a portion of the in-phase perturbation signal (used as the command to the voltage clamp system) into the current measuring amplifier. This procedure is equivalent to placing an ohmic resistor across the membrane (Fishman, Poussart & Moore, 1975). From the resulting solid curves in the left-hand side of Fig. 3, it is evident that with the simulated positive conductance across the membrane, the total admittance behavior now produces the antiresonance observed in Fig. 1 (curve *2*). Thus the admittance depends critically upon whether the net shunt conductance is negative or positive. As a further check of this condition, the admittance was calculated from the ℓHH model with $\bar{g}_K = 0$ and $g_L = 0.3$ mS/cm^2 to obtain the dashed curves in the right-hand side of Fig. 3. Then the admittance was recalculated with $g_L = 9$ mS/cm^2 to obtain the solid curves. As can be seen, the increased positive shunt produced by increasing g_L reproduces the behavior of the real axon and substantiates the complicated effects that can be produced by a negative conductance shunting a resonant system.

3. Anomalous Resonance in the Na Admittance

Another interesting feature of the data in Fig. 2 occurs in the -10 and -30 mV curves. In the frequency range between 10 and 100 Hz the $|Y|$ data show a bump and the data exceed 180°. As discussed earlier, a steady-state, shunt negative conductance is apparent here and caution is required in making interpretations. Since the ℓHH model was useful in accounting for data under these conditions (Fig. 3), calculations were made of the admittance of the Na^+ conductance system by itself, i.e., Y_{Na}, and in combination with an assumed ideal membrane capacitance of 1 μF/cm^2, i.e., $Y_C + Y_{Na}$. These calculations are shown in Fig. 4. In the ℓHH model calculations shown in Fig. 4, the Na^+ inactivation parameter, h, was allowed to take values determined by potential; however,

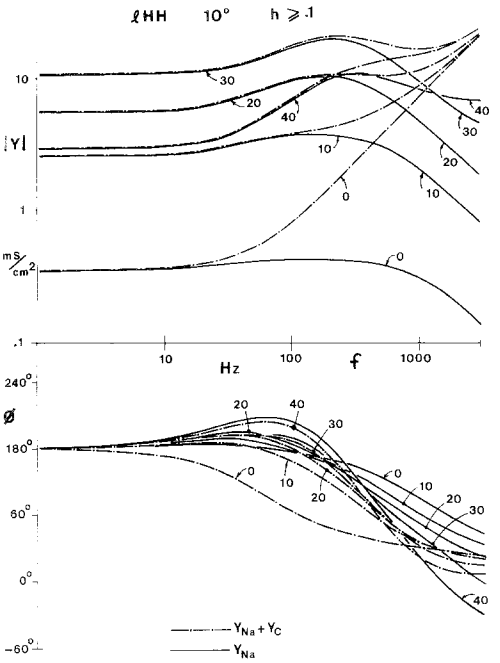

Fig. 4. Calculation of the complex admittance of Na^+ conduction by itself, Y_{Na}, and with added dielectric capacitance, $Y_{Na}+Y_C$ from the ℓHH model at various potential deviations from -60 mV. $\bar{g}_K=g_L=0$ has been assumed. Below 200 Hz the admittance reflects mainly Y_{Na}, i.e., the frequency dependent Na^+ conduction dominates over dielectric capacitance in the total admittance. Also Y_{Na} shows anomalous resonance by itself due to the net negative shunt conductance ($\phi > 90°$) together with the frequency dependent ion conductances

the minimum value was restricted to 0.1. This is consistent with the observation that 290 mM CsF perfusion has the effect of partially removing Na^+ inactivation. These calculations show that at frequencies below 100 Hz the admittance is essentially Y_{Na} with very little contribution from the capacitance. From Y_{Na} at depolarized potentials it is also seen in Fig. 4 that Y_{Na} undergoes a resonance phenomenon by itself. This prediction from the ℓHH model is substantiated by the data in Fig. 2 at potentials of -10 and -30 mV, where the bump below 100 Hz can now be interpreted as a manifestation of this anomalous *resonance* in the admittance of the Na^+ conduction system. A comparison of the phase functions of Y_{Na} computed in Fig. 4 and the measured ones in Fig. 2 also support the interpretation that the anomalous resonance is a consequence of the negative shunt conductance since the low frequency phase exceeds 180° in both cases.

4. Membrane Capacitance Measurement at Low Frequencies by Shunt Conductance Neutralization

Returning to Fig. 2, the -60 mV admittance functions are quite interesting since the $|Y|$ is nearly a straight line and the phase function is a constant 90° at frequencies below several hundred Hz. This behavior can be interpreted only as that of a pure capacitance. In other words, at this potential and these conditions, the membrane appears to reflect only its capacitive character instead of being dominated by the usual conductance effects. Since it has already been shown that a negative shunt conductance is generated during Cs^+ perfusion, it appears as though, at this potential, the shunt negative conductance of the Na^+ system has neutralized the net shunt positive conductance from leakage while the hyperpolarized potential (relative to a rest potential of -37 mV) has made the contribution to the admittance of the time-varying portion of Na^+ conduction negligible. Thus the admittance reflects pure capacitive behavior. To confirm this interpretation, we return again to the ℓHH model for computations. In Fig. 5, with $\bar{g}_K=0$ at $V=0$ (corresponding to -60 mV in Fig. 2), Y_{Na} shows nearly a flat $|Y|$ function and 180° phase for frequencies below 100 Hz, which is indicative of a shunt negative conductance. The addition of membrane capacitance to the admittance, i.e., Y_C+Y_{Na}, yields the same low frequency behavior with capacitive effects becoming significant above 10 Hz. Finally, a positive shunt leakage conductance is added to the total admittance to give $Y_C+Y_L+Y_{Na}$. As can be seen in Fig. 5, as g_L is increased from 0.3 to 0.4 mS/cm^2 there is a remarkably sensitive change in the character of the admittance, which is best interpreted from the phase functions. At $g_L=0.3$ mS/cm^2, the phase at low frequencies is still 180°, indicating a net negative shunt conductance. An increase in g_L to 0.35 mS/cm^2 produces a phase function that stays close to 90°, indicating that the negative shunt conductance has been neutralized by the increased positive g_L. Finally for $g_L=0.4$ mS/cm^2, the net shunt conductance is positive and the phase function reflects the behavior of a parallel RC circuit with phase change from $0\rightarrow 90°$. In comparing Fig. 5 with the data at -60 mV in Fig. 2, it appears that the ℓHH model shows more contribution from the time-varying part of the ionic conductance than in the real axon since the phase function for $g_L=0.35$ mS/cm^2 is not a constant 90° as in the data. Thus it appears that in the real axon at -60 mV the contribution to the admittance from the time variation of the Na^+ system is not significant with respect to the negative shunt conductance

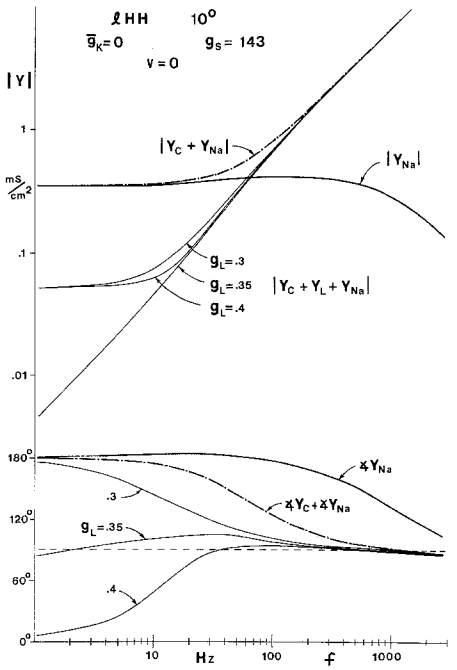

Fig. 5. HH calculation of the complex admittance of Na^+ conduction with added dielectric capacitance (ideal) $Y_{Na}+Y_C$, at $V=0$ corresponding to an absolute membrane potential of -60 mV. For a particular value of leakage conductance, $g_L=0.35$ mS/cm^2, the negative conductance from Y_{Na} is neutralized and $Y=Y_C+Y_L+Y_{Na}$ reflects essentially Y_C. Compare -60 mV curves in Fig. 2

and positive leakage. As a consequence of the neutralization of the positive and negative shunt conductances, a unique situation occurs in which the membrane capacitance dominates the low frequency admittance instead of the usual situation in which the admittance is dominated by ion conduction. Thus, if the above interpretations are correct and there is negligible contribution to the phase by the time varying portion of the Na^+ system, these data suggest that the membrane capacitance has a 90° phase angle in contrast to the "constant phase angle" ($<90°$) behavior for the squid axon previously measured at intermediate frequencies (Curtis & Cole 1938; Cole, 1976).

Discussion

The Features of Y_{Na} and Y_K that Distinguish Na^+ from K^+ Conduction in the ℓHH Model

The admittance data in this paper have been compared to calculations from the ℓHH model with the appropriate parameter changes that corre-

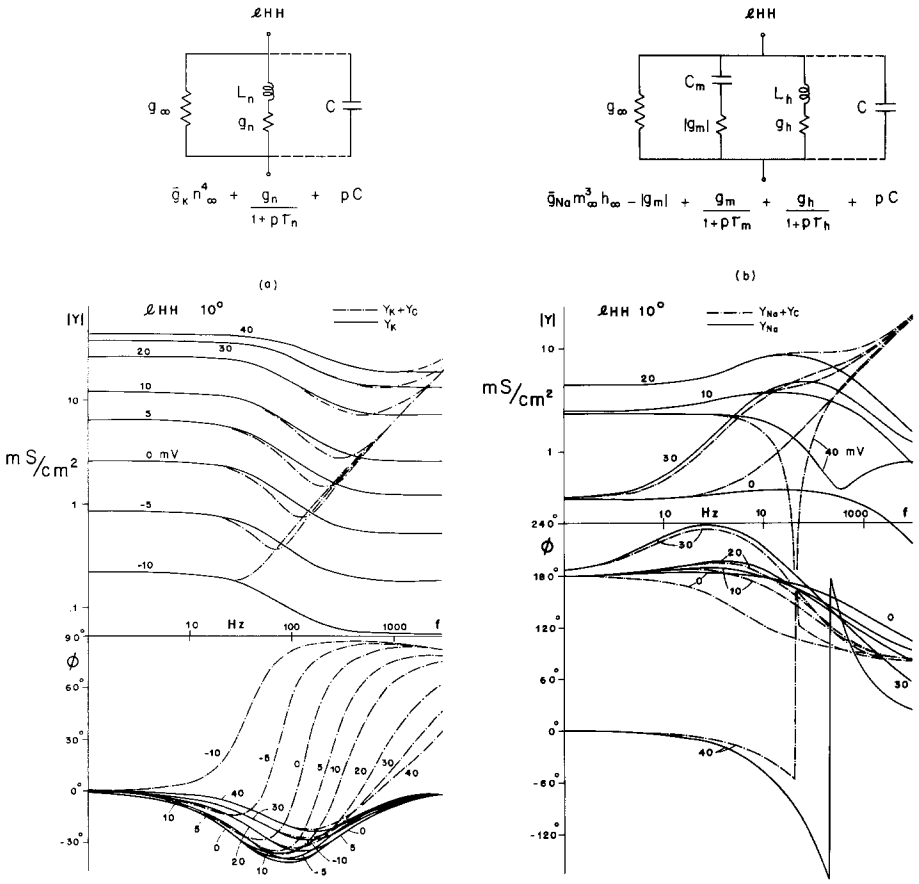

Fig. 6. Calculation of the complex admittance at various membrane potentials (deviations from −60 mV) from the ℓHH model (*a*) K^+ conduction alone, Y_K, and together with dielectric capacitance (ideal), $Y_K + Y_C$ (*b*) Na^+ conduction alone, Y_{Na}, and with capacitance, $Y_{Na} + Y_C$. Circuit above (*a*) is a realization of $Y_K + Y_C$ with expression for each branch below. Circuit above (*b*) is a realization of $Y_{Na} + Y_C$ with expression for each branch below. (Fishman *et al.*, 1977*c*). For K^+ conduction, modified HH values were used according to aforementioned reference; for Na^+ conduction standard HH values were used. *Note:* Y_K is first order (Lorentzian), whereas $Y_K + Y_C$ produces antiresonance (2nd order) due to opposite susceptive elements L_n and C. Y_{Na} is quite complicated by itself, contributing a $g<0$ element as well as two opposite susceptive elements C_m and L_h. Because of the negative g, both $|Y|$ and ϕ must be measured in order to characterize Y_{Na}

spond to the experimental conditions of measurement. On the basis of the comparison we would conclude that the ℓHH model is capable of producing and accounting for all of the significant features which have been observed. Therefore it is instructive to examine computations of the admittance of the Na^+ and K^+ conduction systems from the ℓHH model before proceeding to a discussion of the data. Figure 6 contains sets of admittance calculations (a series resistance of $7\Omega \cdot cm^2$ has been assumed) for

the K^+ and Na^+ conduction processes (solid curves) as well as their modification when membrane capacitance (assumed to be ideal and 1 μF/cm^2) is included (interrupted curves). The leakage conductance has been omitted from these calculations since only the essence of K^+ and Na^+ conduction is desired. In Fig. 6*a*, the circuit realization (*see* Fishman *et al.*, 1977*c*) of the ℓHH Y_K shows a parallel combination of shunt (chord) conductance, $\bar{g}_K n_\infty^4$, and frequency dependent conductance, $g_n(1+p\tau_n)^{-1}$, represented as an inductance-conductance, $L_n g_n$, branch. The computations of $|Y_K|$ at various potentials (rest = 0 mV) have incorporated parameter changes for the K^+ system determined in previous measurements (Fishman *et al.*, 1977*c*). The $|Y_K|$ curves are essentially Lorentzian functions that reflect the frequency dependent term $g_n(1+p\tau_n)^{-1}$, which arises from the first order description for n in the HH formulation. At each potential the Y_K falls from a low frequency asymptotic value to a high frequency asymptotic value that is determined by the K^+ chord conductance, $\bar{g}_K n_\infty^4$. The addition of a parallel membrane capacitance modifies Y_K to produce antiresonance behavior as a consequence of the two opposite susceptances in parallel; L_n from the K^+ conduction and C from the dielectric. It is important to emphasize at this point that the admittance $Y_K + Y_C$ reflects a second order (antiresonance) process although Y_K alone is first order.

In Fig. 6*b*, the circuit realization of the ℓHH Y_{Na} consists of a parallel combination of shunt (chord) conductance, $\bar{g}_{Na} m_\infty^3 h_\infty^- |g_m|$, and two frequency dependent branches (i) $g_m(1+p\tau_m)^{-1}$ represented as a capacitance-conductance, $C_m|g_m|$, branch and (ii) $g_h(1+p\tau_h)^{-1}$ represented as an inductance-conductance, $L_h g_h$, branch. The $-|g_m|$ term in the shunt conductance as well as the $C_m|g_m|$ branch arise from the fact that $g_m < 0$ for $V_K < V < V_{Na}$ (Fishman *et al.*, 1977*c*). The computation of Y_{Na} at various potentials (new rest 20 mV) were made with standard HH parameters (except for $T = 10°$, $Q_{10} = 3$ assumed) for the Na^+ system. In contrast to $|Y_K|$, $|Y_{Na}|$ is not a simple Lorentzian for two reasons: (i) there are two opposite susceptive elements C_m and L_h, in the representation of the Na^+ conduction system because it is second order (this results from the linearization of the product of m^3 and h in the HH formulation) and (ii) $g_m < 0$. Condition *i* by itself would normally produce antiresonance in Y_{Na} as it did when Y_C was added to Y_K (Fig. 6*a*, interrupted curves). However, at the potentials 0, 10, 20 and 30 mV (Fig. 6*b*), the shunt conductance is negative, i.e., $|g_m| > \bar{g}_{Na} m_\infty^3 h_\infty$, since $\phi \to 180°$ as $f \to 0$. Consequently, $|Y_{Na}|$ shows resonance (a local maximum in $|Y_{Na}|$) instead of the expected antiresonance (a local minimum) at these poten-

tials and hence the term "anomalous" resonance to describe this situation. At $V=40$ mV, the shunt conductance becomes positive, i.e., $|g_m| < \bar{g}_{Na} m_\infty^3 h_\infty$, since $|Y_{Na}|$ at this potential shows an antisersonance and $\phi \to 0$ as $f \to 0$. The addition of Y_C to Y_{Na} does not alter the low frequency (<100 Hz) characteristics previously described when the net shunt conductance is negative, but at $V=40$ mV it does shift the antiresonance to a lower frequency and makes it sharper. Since Y_{Na} is exquisitely sensitive to the sign of the net shunt conductance, it is clear that in real measurements of Y_{Na} both leakage conductance as well as any residual conduction left after suppression of $\bar{g}_K$ will produce important effects. These are discussed in the subsequent section.

Separation of Y_{Na} from Y_K in Y Measurements

Measurements of the low frequency admittance in the squid axon in previous publications (Fishman *et al.*, 1977*c*; Poussart *et al.*, 1977) provided detailed, linear data with respect to K^+ conduction and in this paper with respect to Na^+ conduction. The admittance function is a frequency domain characterization of the complete conduction system (including the dielectric properties) and is thus another spectroscopic method. It complements conductance fluctuation spectroscopy in that it is the small signal perturbation counterpart to analysis of conduction fluctuation phenomena that occur spontaneously. As a spectroscopic method, it requires the separation of individual conduction processes in order to facilitate the interpretation of data, as is the case for any macroscopic electrical measurement. Analysis of K^+ conduction, by itself, under normal experimental conditions is relatively simple because TTX is so highly specific and effective in eliminating Na^+ conduction without altering K^+ conduction. However, measurements of the normal Na^+ system alone, in the squid axon, are difficult to obtain because of complexities arising from the stability and control of the axon under these conditions, and because there is no substance that eliminates K^+ conduction in the way that TTX eliminates Na^+ conduction. Although internal application of quarternary ammonium (QA) compounds produces suppressed K^+ conduction conditions, QA ions do not totally eliminate K^+ conduction, and they also degrade Na^+ conduction by as much as 30% (*unpublished observations*). In addition, the residual K^+ conduction process that remains after QA application is modified by the modulation of QA binding to K^+ channels as described in noise

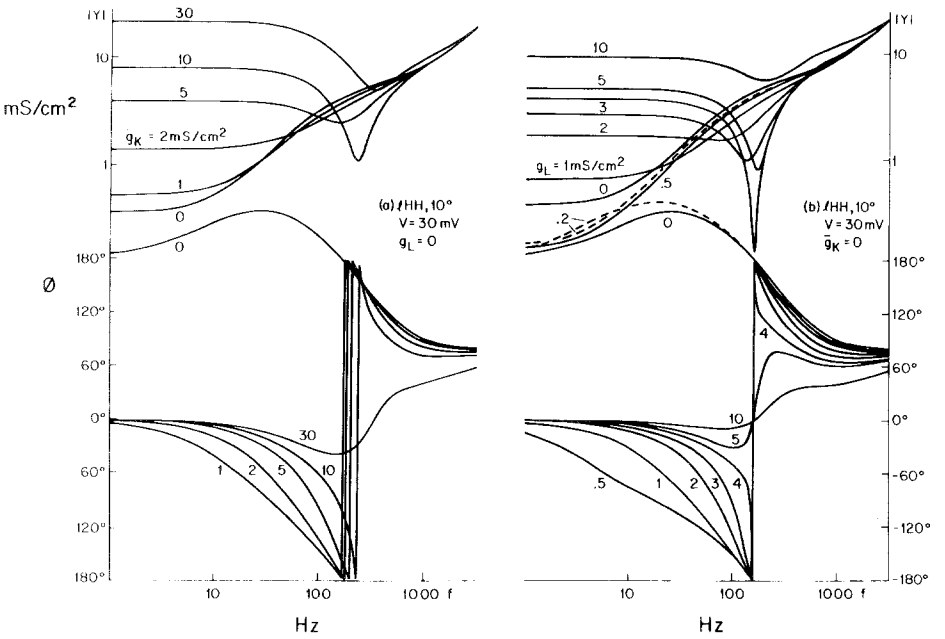

Fig. 7. Calculation of the complex admittance of a squid axon from the ℓHH model at an absolute membrane potential of -30 mV (HH $V=30$) (*a*) for variation in $\bar{g}_K$ ($g_L=0$) to simulate effects of residual K^+ conduction on measurement of $Y_{Na}+Y_C$, and (*b*) for variation in $g_L(\bar{g}_K=0)$ to simulate effects of leakage conduction on measurement of $Y_{Na}+Y_C$. Note complexity of residual K^+ conduction, since it contributes frequency dependent element $g_n(1+n)^{-1}$ as well as a shunt conductance (*see* circuit in Fig. 6*a*). Standard HH values used

analysis (Fishman *et al.*, 1975; 1977*a*; Moore, Fishman & Poussart, 1979). This residual K^+ conduction is extremely critical in noise analysis since it produces fluctuations that exceed and prevent study of the normal Na^+ conduction noise (Moore *et al.*, 1979). It is also important in admittance measurements since the data presented here show that the Na^+ system produces a steady-state negative shunt conductance, and the admittance is drastically altered by contributions to the net shunt conductance from residual K^+ conduction or leakage. To illustrate this last point, Fig. 7 shows computations of the admittance from the ℓHH model at a single potential. In Fig. 7*a* the effect of varying $\bar{g}_K$ ($g_L=0$) is quite dramatic. At $\bar{g}_K \leqq 2$ mS/cm^2, $|Y|$ shows a bump (indicative of a resonance in Y_{Na}, *see* Fig. 2), whereas for $\bar{g}_K > 2$ mS/cm^2 an antiresonance occurs with a shape that is dependent on $\bar{g}_K$. The ϕ functions also reflect frequency dependent as well as ohmic contributions from K^+ conduction to Y as the value of $\bar{g}_K$ is increased. It should be noted here that the sensitivity of Y to values of $\bar{g}_K$ is dependent on potential in a complicated

way so that, at more depolarized potentials than those in Fig. 7*a*, residual K^+ conduction (i.e., $\bar{g}_K < 0.1$ mS/cm^{-2}) can produce substantial changes in Y. If, in addition, the residual K^+ conduction kinetics are altered, such as in the case of QA ions, the separation of Y_{Na} from a measured Y is hopelessly complicated. Thus, as we have emphasized (Fishman *et al.*, 1977*a*), ion channel blocking substances are only useful in studying noise (and now Y) of a particular intrinsic conduction process if they bind so tightly that both the mean and noise currents through the specific channel are suppressed. TTX falls into this category, whereas QA ions as well as other macroscopic K^+ current blockers such as 4-aminopyridine (Fishman *et al.*, 1977*a*) do not. Consequently, we have chosen to study Na^+ conduction by reducing $[K_i^+]$, or replacing it entirely with an impermeable ion such as Cs^+ (Figs. 1 and 2). However, while replacement of $[K_i^+]$ by Cs^+ eliminates outward K^+ conduction, it alters Na^+ conduction by partially removing inactivation. This condition also often exacerbates inadequacies in the spatial control of the preparation. Figure 7*b* shows the effect of increasing a purely ohmic leakage on $|Y|$ with $\bar{g}_K = 0$ and at the same potential and temperature as Fig. 7*a*. Again the response can be either an anomalous resonance (bump) or an antiresonance, depending on the value (in this case between 0.2 and 0.5 mS/cm^2) of g_L that neutralizes the negative shunt conductance. In comparing curves in Fig. 7*a* and *b* at the same value of $\bar{g}_K$ and g_L (e.g., 5 mS/cm^2), it is seen that variation of $\bar{g}_K$ affects Y differently from variation of g_L in that K^+ conduction contributes not only a shunt conductance $\bar{g}_{K_\infty^4}$ but also the frequency dependent term $g_n (1+p\tau_n)^{-1}$ (Fig. 6*a*). It is the latter term that accounts for the difference in the effect of $\bar{g}_K$ or g_L variation, which is indicated by the frequency at which $\phi = \pm 180°$ (*see* Fig. 7 for discontinuity in ϕ). In the case of g_L variation this frequency is constant, whereas in the case of $\bar{g}_K$ variation it varies.

In light of the above discussion, a feature in the computational ℓHH axon can be explained. At a potential of 22 mV depolarized from rest, the ℓHH admittance shows an anti-resonance (*see* Fig. 11, Poussart *et al.*, 1977) which is distinguishable from the anitresonance that occurs at any other potential in the following respects: (i) $|Y|$ at the frequency of resonance. Usually this behavior is not observed in axons (*see* Fig. and the antiresonance is very sharp, (ii) $\phi \to \pm 180°$ at the frequency of resonance. Usually this behavior is not observed in axons (*see* page 6, Poussart *et al.*, 1977). The explanation relates to the interplay of the positive g_L and g_K and negative g_{Na} shunt conductances. At a depolarization of about 20 mV from rest, the sodium system contributes sub-

stantially to the total admittance and can also contribute to a very sharp antiresonance (as in Fig. 3) if the shunt conductance neutralization is nearly complete. Apparently for most axons this neutralization is not complete since g_L and g_K dominate, and thus, the exaggerated antiresonance is not observed at depolarized potentials.

Ion Conduction Processes Dominate Y at Low Frequencies

Takashima and collaborators (Takashima, Yantorno & Pal, 1975; Takashima, 1976; Takashima & Yantorno, 1977; Takashima, Yantorno & Novack, 1977) have measured the high frequency (0.5–50 kHz) admittance of squid axon. They report that the capacitance and conductance as functions of frequency derived from bridge measurements vary with potential. In addition, a capacitive susceptance increase was measured with depolarization that does not occur when tetrodotoxin is used to block Na^+ conduction. It is important to mention that Takashima and coworkers call these functions "membrane capacitance" and "membrane conductance" whereas, in fact, they are measuring the membrane admittance $Y(f)=G(f)+jB(f)$. Thus "membrane conductance" is actually $G(f)=\mathrm{Re}[Y(f)]$ and "membrane capacitance" $C(f)=B(f)/\omega=\mathrm{Im}[Y(f)/\omega]$, where Re and Im denote the "real" and the "imaginary" part of the specified function of ω. As noted previously (Fishman *et al.*, 1977*c*), neither of these functions can be given physical significance without a model. For example, the ℓHH admittance (Chandler, FitzHugh & Cole, 1962; Mauro *et al.*, 1970)

$$Y(p)=C^*p+g_\infty+\frac{g_n}{1+p\tau_n}+\frac{g_m}{1+p\tau_m}+\frac{g_h}{1+p\tau_h}$$

when converted to the form of real plus imaginary parts becomes

$$Y(j\omega)=g_\infty+\frac{g_n}{1+(\omega\tau_n)^2}+\frac{g_m}{1+(\omega\tau_m)^2}+\frac{g_h}{1+(\omega\tau_h)^2}$$
$$+j\omega\left[C^*-\frac{g_n\tau_n}{1+(\omega\tau_n)^2}-\frac{g_m\tau_m}{1+(\omega\tau_m)^2}-\frac{g_h\tau_h}{1+(\omega\tau_h)^2}\right].$$

It is apparent from the above expression that the capacitance function which Takashima *et al.* measure is not solely membrane capacitance C^* but also includes terms involving the frequency domain variation of the ion conductances. It is important to make this distinction because

the basic measurement is that of the complex admittance of the membrane (assuming no artifacts from the measurement set up), and interpretations follow only after a physical model has been assumed. Thus Takashima and co-workers observed that the capacitance change with depolarization is greatest at the low frequency limit (500 Hz) of their measurements. This is due to the fact that at low frequencies the imaginary part of the admittance as well as the real part is dominated by the ion conduction processes. This is further substantiated by the fact that after application of TTX the increase in the low frequency capacitance (i.e., $\mathrm{Im}[Y(f)/\omega]$ with depolarization is abolished. These points also serve to reemphasize that it is the low frequency admittance which contains information about the linear properties of ion conduction.

Y_{Na} is neither a Positive Real nor a Minimum Phase Function; Both $|Y|$ and ϕ must be Determined

In linear network theory (Weinberg, 1962) a driving point function such as the input admittance of a squid axon can be synthesized as a physical network of passive (no energy sources) electrical elements only if it is a positive real (*p.r.*) function. That is, (i) the function $Y(p)$ is real for p real and (ii) the real part of $Y(p) \geqq 0$ for real $p \geqq 0$. It is clear that Y_{Na} in the squid axon is not a *p.r.* function since the data show a steady state negative conductance to be a part of the Na^+ conduction admittance. The ℓHH expression for Y_{Na} in the potential range $V_K < V < V_{Na}$ is

$$Y_{Na} = \bar{g}_{Na} m_\infty^3 h_\infty - |g_m| + \frac{g_m}{1+p\tau_m} + \frac{g_h}{1+p\tau_h}.$$

Since $g_m < 0$ in this potential range, the ℓHH model also yields a Y_{Na} function that is not *p.r.* In this particular case the negative conductance appears as a shunt element and can be removed in order to deal with a *p.r.* function for modeling purposes. However, in systems in which the origin of the negative conductance is unknown, this procedure may not be possible.

Another important aspect of the Y_{Na} function pertains to the determination of Y_{Na} from a given part of the function. All complex functions that are *p.r.* are called conjugate functions since their real and imaginary parts are related and consequently cannot be specified independently. If, for example, either the real or imaginary part of a *p.r.* function

is known analytically or specified graphically then the other part can be obtained by use of the Kronig-Kramers integrals (Cole & Cole, 1941) or the equivalent Hilbert transforms (Guillemin, 1949). This is not the case for a non-*p.r.* function since the function is non-minimum phase in that the ϕ function cannot be predicted or calculated from the $|Y|$ function and vice versa. This can be seen in Fig. 2, for the -10, -30 and -50 mV curves, where ϕ could not be predicted from $|Y|$. Thus in the case of a non-minimum phase function, such as Y_{Na}, it is necessary to measure the entire complex function, i.e., both $\mathrm{Re}[Y_{Na}]$ and $\mathrm{Im}[Y_{Na}]$ or $|Y|$ and ϕ, in order that the data be useful and informative. For example, in Fig. 2 without the function, in which $\phi \geqq 180°$, it would be impossible to know that $|Y|$ reflects a negative conductance.

The Phase Angle of Membrane Admittance at Low Frequency after Conductance Neutralization

The first impedance measurements on the squid axon (Curtis & Cole, 1938) indicated that the dielectric portion of the axon was lossy. The non-ideal nature of the dielectric continues to be a problem with respect to interpretations of voltage clamp currents. The capacitive current transient after a step change in membrane potential deviates significantly from a simple exponential (Hodgkin, Huxley & Katz, 1952; FitzHugh & Cole, 1973); first decaying more rapidly and then more slowly than an exponential. Consequently, early (10–100 μsec) as well as longer time estimates of leakage current are contaminated by the non-ideal capacitive response (Fishman, 1970; Moore *et al.*, 1970). Furthermore, as pointed out by FitzHugh and Cole (1970), proper compensation for series resistance cannot be made without accounting for the non-ideal capacitive response.

Cole (1932) showed that the impedance locus (Cole & Cole, 1941, plot) for a variety of tissues is described by a semicircle with a center located off the real axis. The half angle ϕ between radii from the center of the semicircle to the zero and infinite frequency resistances is equivalent to the asymptotic phase angle of the preparation as $f \to \phi$. For an ideal capacitor with no loss ($\phi = 90°$), the center of the semicircle is on the real axis, and the impedance locus at high frequency is normal to the real axis. However, in the case of a non-ideal (lossy) capacitance the asymptotic value of the phase angle at high frequency approaches a constant that is somewhat less than the expected value of 90° for an

ideal capacitance. Thus Cole has denoted this effect as the "constant phase angle impedance." Various attempts have been made to explain this effect but none have been successful (Taylor, 1965).

As discussed in the previous section, the low frequency admittance of squid axon is usually dominated by the frequency dependent behavior of the ion conductances. However, after suppression of K^+ conduction, the Na^+ conduction system contributes a negative conductance that can neutralize the residual (leakage) positive conductance. Furthermore, at a hyperpolarized membrane potential the neutralization persists while the frequency dependent terms $g_m(1+p\tau_m)^{-1}$ and $g_h(1+p\tau_h)^{-1}$ become very small. This latter statement was verified by calculations on the ℓHH model in which the phase angle for $|Y_{Na}|$ at absolute membrane potentials of -65 to -70 mV (similar to Fig. 5) is a constant 180° from 1 to 100 Hz and then decreases to about 140° at 1 kHz. The $|Y_{Na}|$ for the same calculation yields a nearly flat function out to 400 Hz and then declines very slowly to 1 kHz. Thus according to the ℓHH model at potentials hyperpolarized from rest, Y_{Na} behaves like a pure negative conductance out to 100 Hz. Furthermore, the possibility of a contribution to the admittance measurement from the movement of "gating" charges has been excluded previously (Fishman *et al.*, 1977*c*). Consequently, it would appear that the 90° phase angle observed at -60 mV in Fig. 2 out to 100 Hz reflects the phase angle of the dielectric and suggests that membrane capacitance is not lossy, at least when measured at low frequencies and with only negligible ion currents.

The most obvious interpretation of this result is that the constant phase angle impedance is a consequence of preparation and measurement complexities. It has been known for some time that the phase angle of artificial lipid bilayers at high frequencies is 90° (Hanai, Haydon & Taylor, 1965), and G. Szabo (*personal communication*) has recently reconfirmed this in very accurate admittance measurements. In addition, marine eggs produce 90° (Cole & Spencer, 1938). As Cole (1972) notes in his description of early measurements of *Arbacia* eggs, he measured $\phi < 90°$, but as the volume and thus number of eggs in the suspension was reduced to a single egg, $\phi = 90°$ was obtained. Thus, the $\phi < 90°$ found in multicellular preparations and tissues may be due to a distribution of time constants from a population of cell sizes except that a very broad distribution is to be explained. But how could this explain the constant phase angle in single cells and in particular the squid axon? The fact is that there are few preparations in which an uncomplicated membrane can be measured. The Schwann cell layer has added enormous

complexity to the squid axon. Cole (1976) has shown that this layer adds a series impedance (and perhaps a distributed one) to the membrane instead of a resistance. Could the constant phase angle at high frequency result from these access pathways? Alternatively, the 90° phase angle measured at low frequencies during negligible ion current flow and conductance neutralization suggests that the occurrence of a phase angle of less than 90°, which is normally measured at intermediate frequencies during ion conduction, may be due to conducting structures in the membrane. This suggestion could be checked relatively easily by blocking the ion conductances and measuring the phase angle at intermediate frequencies.

We thank Dr. Rita Guttman for comments on the mansucript. This work was supported in part by NIH grants NS-11764, NS-13778, NS-13520 and Canadian Research Council grant A-5274.

References

Chandler, W.K., FitzHugh, R., Cole, K.S. 1962. Theoretical stability properties of a space-clamped axon. *Biophys. J.* **2**:105

Cole, K.S. 1932. Electric phase angle of cell membranes. *J. Gen. Physiol.* **15**:641

Cole, K.S. 1972. Membranes, Ions and Impulses. (Revised ed.) University of California Press, Berkeley [First published in 1968]

Cole, K.S. 1976. Electrical properties of the squid axon sheath. *Biophys. J.* **16**:137

Cole, K.S., Cole, R.H. 1941. Dispersion and absorption in dielectrics. I. Alternating current characteristics. *J. Chem. Phys.* **9**:341

Cole, K.S., Spencer, J.M. 1938. Electric impedance of fertilized *Arbacia* egg suspensions. *J. Gen. Physiol.* **21**:583

Cole, R.H. 1977. Dielectric theory and properties of DNA in solution. *Ann. N.Y. Acad. Sci.* **303**:59

Curtis, H.J., Cole, K.S. 1938. Transverse electric impedance of the squid giant axon. *J. Gen. Physiol.* **21**:757

Fishman, H.M. 1970. Leakage current in the squid axon membrane after application of TTX and TEA. *Biophys. Soc. Abstr.* 109*a*

Fishman, H.M. 1975. Complex impedance measurements of squid axon membrane via input-output cross correlation function. *In*: Proc. 1st Symp. on Testing and Identification of Nonlinear Systems. G.D. McCann and P.Z. Marmarelis, editors. pp. 257–274. California Institute of Technology, Pasadena

Fishman, H.M., Moore, L.E., Poussart, D.J.M. 1975. Potassium-ion conduction noise in squid axon membrane. *J. Membrane Biol.* **24**:305

Fishman, H.M., Moore, L.E., Poussart, D. 1977*a*. Ion movements and kinetics in squid axon. II. Spontaneous electrical fluctuations. *Ann. N.Y. Acad. Sci.* **303**:399

Fishman, H.M., Moore, L.E., Poussart, D. 1977*b*. Asymmetry currents and admittance in squid axons. *Biophys. J.* **19**:177

Fishman, H.M., Poussart, D.J.M., Moore, L.E. 1975. Noise measurements in squid axon membrane. *J. Membrane Biol.* **24**:281

Fishman, H.M., Poussart, D., Moore, L.E. 1978. Admittance of the Na conduction system in squid axon. *Biophys. J.* **21**:163*a*

Fishman, H.M., Poussart, D.J.M., Moore, L.E., Siebenga, E. 1977*c*. K^+ conduction description from the low frequency impedance and admittance of squid axon. *J. Membrane. Biol.* **32**:255

FitzHugh, R., Cole, K.S. 1973. Voltage and current clamp transients with membrane dielectric loss. *Biophys. J.* **13**: 1125

Guillemin, E.A. 1949. The Mathematics of Circuit Analysis. John Wiley and Sons, New York

Hanai, T., Haydon, D.A., Talyor, J. 1965. The influence of lipid composition and of some adsorbed proteins on the capacitance of black hydrocarbon membrane. *J. Theor. Biol.* **9**:422

Hodgkin, A.L., Huxley, A.F. 1952. A quantitative description of membrane current and its application to conduction and excitation in nerve. *J. Physiol. (London)* **117**:500

Hodgkin, A.L., Huxley, A.F., Katz, B. 1952. Measurement of current voltage relations in the membrane of the giant axon of *Loligo*. *J. Physiol. (London)* **116**:424

Mauro, A., Conti, F., Dodge, F., Schor, R. 1970. Subthreshold behavior and phenomenological impedance of the squid giant axon. *J. Gen. Physiol.* **55**:497

Moore, L.E., Fishman, H.M., Poussart, D. 1979. Chemically induced K^+ conduction noise in squid axon. *J. Membrane Biol.* **47**:99

Moore, J.W., Narahashi, T., Poston, R., Arispe, N. 1970. Leakage currents in squid axon. *Biophys. Soc. Abstr.* 180*a*

Poussart, D., Moore, L.E., Fishman, H.M. 1977. Ion movements and kinetics in squid axon: I. Complex admittance. *Ann. N.Y. Acad. Sci.* **303**:355

Takashima, S. 1976. Membrane capacity of squid giant axon during hyper- and depolarizations. *J. Membrane Biol.* **27**:21

Takashima, S., Yantorno, R. 1977. Investigation of voltage-dependant membrane capacity in squid axon. *Ann. N.Y. Acad. Sci.* **303**:306

Takashima, S., Yantorno, R., Novack, R. 1977. Dipole moment changes and voltage dependent membrane capacity of squid axon. *Biochim. Biophys. Acta* **469**:74

Takashima, S., Yantorno, R., Pal, N.C. 1975. Electrical properties of squid axon membrane. II. Effect of partial degradation by phospholipase A and pronase on electrical characteristics. *Biochim. Biophys. Acta* **401**:15

Taylor, R.E. 1965. Impedance of squid axon membrane. *J. Cell Comp. Physiol.* **66 (Suppl. 2)**:21

Weinberg, L. 1962. Network Analysis and Synthesis. McGraw-Hill, New York